BIOCHEMISTRY
including biophysical chemistry & molecular biology

Article

pubs.acs.org/biochemistry

Kinetic and Structural Evaluation of Selected Active Site Mutants of the *Aspergillus fumigatus* KDNase (Sialidase)

Juliana H. F. Yeung,[†] Judith C. Telford,[§] Fahimeh S. Shidmoossavee,[‡] Andrew J. Bennet,[‡] Garry L. Taylor,[§] and Margo M. Moore*[,†]

[†]Department of Biological Sciences and [‡]Department of Chemistry, Simon Fraser University, Burnaby, British Columbia V5A 1S6, Canada

[§]BSRC, University of St Andrews, St Andrews, Fife KY16 9ST, U.K.

Supporting Information

ABSTRACT: *Aspergillus fumigatus* is an airborne fungal pathogen. We previously cloned and characterized an *exo*-sialidase from *A. fumigatus* and showed that it preferred 2-keto-3-deoxynononic acid (KDN) as a substrate to *N*-acetylneuraminic acid (Neu5Ac). The purpose of this study was to investigate the structure−function relationships of critical catalytic site residues. Site-directed mutagenesis was used to create three mutant recombinant enzymes: the catalytic nucleophile (Y358H), the general acid/base catalyst (D84A), and an enlargement of the binding pocket to attempt to accommodate the *N*-acetyl group of Neu5Ac (R171L). Crystal structures for all enzymes were determined. The D84A mutation had an effect in decreasing the activity of AfKDNase that was stronger than that of the same mutation in the structurally similar sialidase from the bacterium *Micromonospora viridifaciens*. These data suggest that the catalytic acid is more important in the reaction of AfKDNase and that catalysis is less dependent on nucleophilic or electrostatic stabilization of the developing positive charge at the transition state for hydrolysis. Removal of the catalytic nucleophile (Y358H) significantly lowered the activity of the enzyme, but this mutant remained a retaining glycosidase as demonstrated by nuclear magnetic resonance spectroscopic analysis. This is a novel finding that has not been shown with other sialidases. Kinetic activity measured at pH 5.2 revealed that R171L had higher activity on a Neu5Ac-based substrate than wild-type KDNase; hence, leucine in place of arginine in the binding pocket improved catalysis toward Neu5Ac substrates. Hence, whether a sialidase is primarily a KDNase or a neuraminidase is due in part to the presence of an amino acid that creates a steric clash with the *N*-acetyl group.

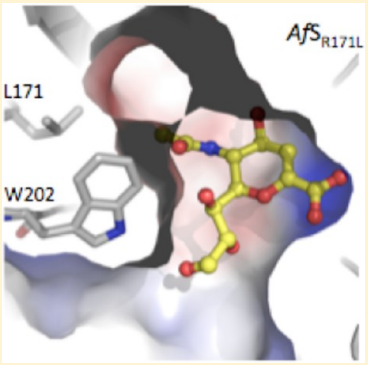

Aspergillus species are filamentous fungi that have emerged as a cause of serious disease in patients with underlying medical conditions such as cystic fibrosis or immune suppression.[1] *Aspergillus fumigatus* is the most prevalent airborne fungal pathogen in developed countries and is responsible for approximately 90% of life-threatening cases of invasive pulmonary aspergillosis in immunocompromised patients.[2] The first step of *A. fumigatus* pathogenesis is inhalation of airborne conidiospores (conidia) by a susceptible individual followed by attachment of conidia to lung tissue proteins.[3] Glycans on the surface of *A. fumigatus* conidia contain terminal *N*-acetylneuraminic acids (Neu5Ac) that are α2,6-linked to underlying galactose residues. These sialic acids are responsible in part for mediating the attachment of conidia to host lung cells and basal lamina proteins such as fibronectin.[4,5] The removal of conidial sialic acids significantly decreased the rate of uptake of spores by cultured murine macrophages and type 2 pneumocytes compared to controls.[5] These data indicate that sialylated molecules on the conidial surface act as ligands for both professional and nonprofessional phagocytes.

Although sialic acids are mostly found in higher eukaryotes, they are also found in many species of bacteria,[6−8] fungi,[4,9−11] and protozoans.[7,12,13] These microorganisms, both pathogenic and nonpathogenic, have evolved to synthesize these negatively charged sugars *de novo* or capture them from the environment for use as a carbon or nitrogen source. Some pathogenic microorganisms have evolved to use sialic acid by coating themselves in sialic acid to resist components of the host innate immune response.[7,13,14] In addition, certain pathogenic bacteria utilize cell surface sialic acids to interact specifically with different host−cell surface receptors;[6] for example, *Campylobacter jejuni*, the bacterium that causes Guillain-Barré syndrome, interacts with host macrophages by binding to sialoadhesins (Siglec-1).[15]

A. fumigatus grown in chemically defined media lacking sources of sialic acid displayed *N*-acetylneuraminic acid (Neu5Ac) on the surface of conidia,[4,5] suggesting that *de novo* synthesis of sialic acid occurs in this fungus. However, sialic acid biosynthetic genes have not yet been identified by us or others in any of the *A. fumigatus* strains sequenced to date.[16] A gene encoding a sialidase (EC 3.2.1.18), a glycosyl hydrolase that cleaves glycosidic linkages of sialic acid, was identified in

Received: August 24, 2013
Revised: November 8, 2013
Published: December 2, 2013

dx.doi.org/10.1021/bi401166f | *Biochemistry* 2013, 52, 9177−9186

the genome sequence of *A. fumigatus*. Subsequent studies revealed that the *A. fumigatus* sialidase was a functional protein that structurally resembled bacterial sialidases.[17]

Many microbial pathogens secrete sialidases, enzymes that hydrolyze sialic acid from oligosaccharides. The released sialic acids are then imported into the cell or directly linked to cell surface glycoconjugates.[7] Sialidases also have an important role in bacterial nutrition.[18,19] Sialidase activity has been identified in other pathogenic fungi such as *Fonsecaea pedrosoi* and *Sporothrix schenckii*.[10,20,21] Compared to bacterial sialidases, the *A. fumigatus* sialidase had lower activity in cleaving Neu5Ac from glycan substrates. Kinetic analysis of the recombinant *A. fumigatus* sialidase (AfKDNase) revealed that its preferred substrate is not Neu5Ac but rather 2-keto-3-deoxy-D-*glycero*-D-*galacto*-nononic acid (KDN), another naturally occurring sialic acid that has an OH group in place of the *N*-acetyl group at C-5.[22] KDN is found in almost all types of glycoconjugates where KDN residues are often in place of Neu5Ac and frequently found among lower vertebrates and bacteria.[23] Very little is known about the catabolism of KDN; however, it was shown that the KDNase-producing bacterium *Sphingobacterium multivorum* used KDN as a sole carbon source.[24] KDNase has also been identified in several species of mollusks and in rainbow trout.[23] To date, the catalytic mechanism of KDNases has not been fully investigated.

The active sites of sialidases and *trans*-sialidases found in viruses, bacteria, and eukaryotes all possess several key features that are essential for catalysis: a strictly conserved cluster of three arginines that bind the carboxylate group of the substrate via electrostatic interactions, a distal glutamate residue that forms a salt bridge with one of the conserved arginine residues,[25] and a tyrosine-glutamic acid dyad and an aspartic acid that act as the general acid/base catalyst. All known natural sialidases catalyze the hydrolysis of the substrate with retention of the anomeric configuration, an observation that is compatible with this family of enzymes operating via a standard double-displacement mechanism.[25−27]

Though all sialidases have a similar tertiary structure, members of this family of enzymes share a low degree of sequence identity. All active sites of sialidases that hydrolyze Neu5Ac have a hydrophobic pocket to accommodate the *N*-acetyl group of the substrate, but the exact residues that form this pocket are generally not conserved. The crystal structure of the recombinant *A. fumigatus* sialidase/KDNase (AfKDNase) showed that the arginine pocket accommodates the smaller hydroxyl group at C-5 in KDN.[22] Comparison of the crystal structure of AfKDNase with *Micromonospora viridifaciens* (bacterial) sialidase (MvS) indicated that the presence of arginine 171 (not part of the triarginine cluster) in place of leucine in this pocket, as in MvS, may prevent rAfS from holding the Neu5Ac substrate in place for efficient catalysis.

Previous mutagenesis work on MvS showed that mutating the critical nucleophilic tyrosine in the active site substantially altered the mechanism of the enzyme by changing it from a retaining to an inverting glycoside hydrolase.[26] Similarly, it has been shown that a natural nucleophilic variant of the TcTS, which is inactive, has a tyrosine to histidine substitution.[28] Interestingly, a mutation of the general acid/base catalyst in MvS from an aspartic acid to a glycine did not affect the function of the enzyme significantly.[29] In this study, we examined the effect of selected active site mutations on the structure and activity of the *A. fumigatus* sialidase/KDNase. Specifically, we examined a mutation of the active site nucleophile (Y358H) and an acid catalyst mutant (D84A) (Figure 1). In addition, we studied the kinetics and structure of the R171L mutant of AfKDNase to determine whether modifying the pocket to resemble that of the *M viridifaciens* sialidase resulted in greater activity in cleaving Neu5Ac compared to KDN.

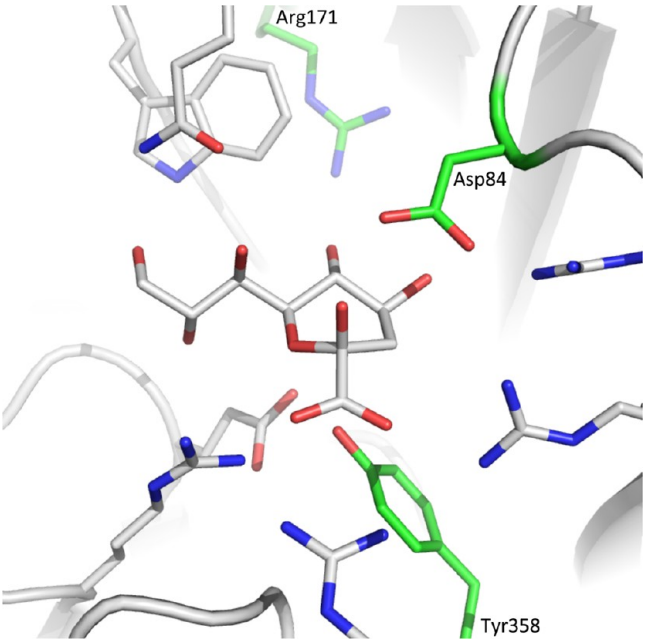

Figure 1. Amino acids in the AfKDNase catalytic domain targeted for site-directed mutagenesis. Two amino acids (Y358 and D84) are believed to be the catalytic nucleophile and the general acid, respectively, that are essential for the hydrolase reaction. The arginine residue (R171) is believed to be the key amino acid reducing the efficiency of Neu5Ac cleavage by AfKDNase.

EXPERIMENTAL PROCEDURES

All chemicals were of analytical grade or better and were purchased from Sigma-Aldrich unless noted otherwise. 8-Fluoro-4-methylumbelliferyl β-D-galactopyranoside [Gal β-FM, **3** (Scheme 1 of the Supporting Information)] was made by following a published procedure.[30] Cytidine 5′-triphosphate disodium salt was purchased from 3B Scientific Corp. Pyrophosphatase from baker's yeast (*Saccharomyces cerevisiae*) was purchased from Sigma-Aldrich. *Escherichia coli* Neu5Ac aldolase was purchased from Codexis, and CMP-Neu5Ac synthase from *Neisseria meningitidis* was expressed according to the literature (not purified).[31] *Photobacterium* sp. JT-ISH-224 α-2,6-sialyl transferase was a kind donation from M. Gilbert (National Research Council, Ottawa, ON). ^{1}H and ^{13}C nuclear magnetic resonance (NMR) spectra were recorded on a Bruker 600 MHz spectrometer, and chemical shifts are given in parts per million and coupling constants (J) in hertz. Melting points were determined on an MPA100 automated melting point system. Optical rotations were measured on a Perkin-Elmer 341 polarimeter and are reported in units of grams per 100 mL.

Expression and Purification of AfKDNase Mutants for Kinetic and Structural Studies. The KDNase gene from *A. fumigatus* clinical isolate ATCC 13073 was originally cloned into the pET28A+ vector (EMD chemicals Inc., San Diego, CA) and expressed in *E. coli* (DE3) cells.[17] Point mutations were introduced via site-directed mutagenesis to generate the

Y358H, R171L, and D84A mutants using the QuikChange Lightning mutagenesis kit (Agilent Technologies). Briefly, *E. coli* cells expressing KDNase in a pET28A+ vector were grown in Luria broth with 50 μg/mL kanamycin at 37 °C, while being shaken at 220 rpm. Once the culture OD_{600} had reached 0.5, protein expression was induced with 0.5 mM IPTG (isopropyl thio-β-D-galactopyranoside) and the sample incubated overnight at room temperature.

Cells were then harvested as previously described.[17] Briefly, *E. coli* cultures were collected by centrifugation at 3000*g* for 20 min at 4 °C. Following lysozyme treatment and sonication, the suspension was centrifuged. The lysate containing the expressed six-His-tagged KDNase was added to 1 mL of nickel-nitrilotriacetic acid agarose (Ni-NTA) (Qiagen), and the KDNase was eluted in 5 mL of elution buffer [50 mM Tris-HCl, 100 mM NaCl, and 20 mM imidazole (pH 8.0)]. Imidazole and nonspecific proteins were removed by gel filtration chromatography (ÄTKAFPLC, GE Healthcare, with Hi-Prep 26/60 Sephacryl S-100H resin and a column size of 320 mL) with cleanup buffer [50 mM Tris-HCl and 100 mM NaCl (pH 8.0)] at 4 °C. Fractions collected were analyzed by 12% sodium dodecyl sulfate−polyacrylamide gel electrophoresis. Selected fractions containing only KDNase were concentrated by using a 30000 molecular weight cutoff centrifugal filter (Millipore, Billerica, MA). The concentrated protein solution was frozen using liquid nitrogen and stored at −80 °C.

Determination of the Optimal pH for Each Mutant. The optimal pH values of the purified enzymes were determined by the amount of 4-methylumbelliferone released from KDN-MU and Neu5Ac-MU by AfKDNase in buffers with varying pH values. The buffers 40 mM sodium formate (pH 3−3.5), 50 mM sodium acetate (pH 4−5), 16 mM sodium tartrate (pH 5.2), 32.5 mM 2-(*N*-morpholino)ethanesulfonic acid (MES) (pH 6−7), 40 mM 3-(*N*-morpholino)propanesulfonic acid (MOPS) (pH 6.5), and 50 mM Tris-HCl (pH 7.5−9) were used. The ionic strength of all buffers was maintained at 100 mM with NaCl, and all buffers were prepared for use at 37 °C. The amount of 4-methylumbelliferone released during the enzyme reaction was detected by a fluorescence microplate reader (SpectraMax M2e, Molecular Devices) at excitation and emission wavelengths of 365 and 450 nm, respectively. The amount of fluorescence detected was adjusted to reflect the molar concentration of the substrate cleaved using standard curves generated with 4-methylumbelliferone (Fluka) over a range of concentrations (1−150 μM) in the different aforementioned pH buffers.

Kinetic Activity Assays. The activities of enzyme preparations were determined by the cleavage of the synthetic sialic acid substrate, 4-methylumbelliferyl α-D-*N*-acetylneuraminic acid (Neu5Ac-MU) (Rose Scientific, Edmonton, AB), 4-methylumbelliferyl α-2-keto-3-deoxynonic acid (KDN-MU), and the α2,6 isomer of 8-fluoromethylumbelliferyl α-2-keto-3-deoxy-D-*glycero*-D-*galacto*-nononylgalactopyranoside (KDNα2,6GalβFMU).

Reaction mixtures with Neu5Ac-MU and KDN-MU were set up in 96-well plates by adding the substrate over a range of concentrations (50−800 μM), purified recombinant enzyme, and the specific reaction buffer for a total volume of 100 μL. In reaction mixtures with KDNα2,6GalβFMU, 200 μM substrate was used. *Aspergillus oryzae* β-galactosidase (Sigma) (0.1%) was added to each mixture. Plates were incubated at 37 °C for 45 min, and the amount of 4-methylumbelliferone released was determined using a fluorescence microplate reader (SpectraMax M2e, Molecular Devices) at excitation and emission wavelengths of 365 and 450 nm, respectively.

Extended kinetic activity experiments were conducted for up to 600 min for reactions with R171L or D84A and KDNα2,6GalβFMU to ensure that enzymatic activity reached completion. Each enzyme reaction mixture had a total volume of 500 μL; each was set up in a quartz cuvette that contained 200 μM substrate and 0.1% *A. oryzae* β-galactosidase (Sigma) in the appropriate reaction buffer. The fluorescence over the course of the reaction was measured using a Cary Eclipse fluorescence spectrophotometer. All kinetic experiments were performed in triplicate. A 50 mM sodium acetate/100 mM sodium chloride buffer was used for kinetic experiments at pH 4.0, and a 16 mM sodium tartrate/100 mM sodium chloride buffer was used for experiments at pH 5.2.

Fluorescence produced during the course of the reaction was related to the concentration of Neu5Ac-MU, KDN-MU, or KDNα2,6GalβFMU cleaved by comparison with a standard curve of 4-methylumbelliferone (Fluka) or 8-fluoro-4-methylumbelliferone (synthesized starting from 2,3,4-trifluoronitrobenzene purchased from TCI America).[30]

Standard curves generated with 4-methylumbelliferone over a range of concentrations (1−150 μM) were made using pH 4.0 and 5.2 buffers, and the standard curve made with 8-fluoro-4-methylumbelliferone at concentrations between 5 and 400 μM was made using pH 4.0 buffer. To ensure the amount of *A. oryzae* β-galactosidase used was sufficient and that the reaction was a zero-order reaction, 0.1% *A. oryzae* β-galactosidase was incubated with 150 and 350 μM 8-fluoro-4-methylumbelliferyl β-D-galactopyranoside (Gal β-FM) and the activity was observed by fluorescence spectrometry using excitation and emission wavelengths of 365 and 450 nm, respectively. The observed results from these experiments did exhibit zero-order enzyme kinetic activity (data not shown); therefore, it was assumed that the reaction with *A. oryzae* β-galactosidase and GalβFMU would not interfere with the reaction between the mutant KDNases and KDNα2,6GalβFMU.

Determination of Retaining or Inverting Activity of the Y358H Mutant by ^{1}H NMR. ^{1}H NMR spectroscopy was used to examine the formation of the product from the hydrolysis of KDN-MU by the Y358H mutant. NMR spectra were recorded on a 600 MHz Bruker spectrometer. The reaction mixture consisted of 0.34 μg of Y358H mutant AfKDNase, 0.01% bovine serum albumin (BSA) (BioShop Canada), and 0.5 mg of KDN-MU, made up to 600 μL with a solution of 20 mM homopiperazine-1,4-bis(2-ethanesulfonic acid) (Santa Cruz Biotechnology, Inc.) at pD 4.0, and placed in a 5 mm NMR tube. Prior to the addition of the enzyme, the magnetic field was manually shimmed and a ^{1}H NMR spectrum was acquired. The magnetic field was reshimmed and retuned after the addition of the enzyme to improve the signal-to-noise ratio. Shimming took ∼15 min, during which the enzyme reaction started. The reaction mixture was incubated at 296 K, and all NMR spectra were recorded continuously over a period of 2 h (16 scans and 2 min per spectrum).

Determination of Crystal Structures of Mutants. Crystals of the mutant proteins were formed and cryoprotected for freezing and X-ray data collection as described previously for wild-type AfS.[22] All data were collected at 100 K in house (Rigaku-MSC Micromax-007 X-ray generator and Saturn 944+ CCD detector). MOSFLM[32] was used to integrate the data; the

Table 1. X-ray Data Collection and Refinement Statistics

	AfS_{D84A}	AfS_{Y358H}	AfS_{R171L}–Neu5Ac2en complex
	Data Collection[a]		
X-ray source	in house	in house	in house
X-ray wavelength (Å)	1.542	1.542	1.542
resolution (Å)	12.4–1.84 (1.94–1.84)	12.4–1.84 (1.94–1.84)	12.4–1.84 (1.94–1.84)
unit cell dimensions			
a (Å)	75.9	75.9	75.9
b (A)	57.8	58.1	58.0
c (Å)	94.6	94.4	94.6
β (deg)	99.9	99.9	99.9
no. of observations	273633	274759	302861
redundancy	2.0 (1.8)	2.2 (1.9)	2.2 (2.0)
completeness (%)	98.9 (94.4)	98.5 (92.0)	99.2 (96.9)
R_{merge} (%)[b]	5.5 (14.2)	8.8 (21.2)	8.6 (27.8)
$I/\sigma I$	18.2 (7.5)	11.0 (5.0)	13.8 (4.2)
	Refinement		
no. of reflections used	70126	65819	66869
no. of atoms	7201	7158	7253
no. of protein atoms	6039	5981	6010
no. of water molecules	1162	1165	1396
no. of ligand atoms	not available	not available	20
average *B* factor (Å^2)	9.9	9.9	12.1
protein	7.5	7.6	9.5
water	22.4	21.8	28.9
ligand	not available	not available	13.5
R factor[c]	0.143	0.173	0.155
R_{free}[d]	0.178	0.224	0.194
root-mean-square deviation in bond lengths (Å)	0.009	0.010	0.009
root-mean-square deviation in bond angles (deg)	1.14	1.24	1.19

[a]Values in parentheses correspond to values for the highest-resolution shell. [b]$R_{merge} = \sum_{hkl}\sum_i |I_{hkl,i} - \langle I_{hkl}\rangle| / \sum_{hkl}\langle I_{hkl}\rangle$. [c]*R* factor = $(\sum||F_o| - |F_c||)/(\sum|F_o|)$. [d]$R_{free} = (\sum||F_o| - |F_c||)/(\sum|F_o|)$. R_{free} was calculated from 5% of the reflections excluded from the refinement.

Table 2. Kinetic Parameters of the *A. fumigatus* Sialidase/KDNase Wild-Type Enzyme and the Three Mutant Enzymes Generated in This Study[a]

sialidase	substrate	k_{cat}/K_m (M^{-1} s^{-1})	substrate	k_{cat}/K_m (M^{-1} s^{-1})
AfKDNase	KDN-MU	$(1.82 \pm 0.09) \times 10^5$[b] (ref 22)	NANA-MU	22.3 ± 3.0[b] (ref 17)
	KDN-MU[b]	47.7 ± 3.6	NANA-MU (pH 5.2)	53.3 ± 4.2
	KDN*α*2,6Gal*β*FMU	$(8.0 \pm 0.6) \times 10^3$		
R171L	KDN-MU	75.2 ± 7.7	NANA-MU	2.3 ± 0.1
	KDN-MU[b]	0.33 ± 0.02	NANA-MU[b]	74.2 ± 1.4
	KDN*α*2,6Gal*β*FMU	1.62 ± 0.04		
Y358H	KDN-MU	26.8 ± 0.9	NANA-MU[b]	14.5 ± 1.1
	KDN*α*2,6Gal*β*FMU	8.9 ± 0.3		
D84A	KDN-MU	11.6 ± 0.6	NANA-MU[b]	19.0 ± 1.7
	KDN*α*2,6Gal*β*FMU	0.2 ± 0.1		
MvS	KDN-Mu	$(1.03 \pm 0.36) \times 10^3$	NANA-MU	$(7.2 \pm 1.4) \times 10^6$[b] (ref 29)

[a]Values obtained with a bacterial (*M. viridifaciens*) sialidase under the same conditions are shown for comparison. [b]Kinetic experiments from this study were performed at pH 5.2 using 16 mM sodium tartrate (pH 5.2) buffer. All other experiments were completed using 50 mM sodium acetate (pH 4.0) buffer, or pH 3.5 (ref 17).

crystals of the mutant proteins were isomorphous with the wild type and belonged to space group $P2_1$.

The apo model [Protein Data Bank (PDB) entry 2XCY] was refined in REFMAC5[33] against data collected for each of the mutant structures (AfS_{Y358H}, AfS_{D84A}, and AfS_{R171L}). For the R171L mutant, crystals were soaked in 500 mM sialidase transition state analogue 2-deoxy-2,3-dehydro-*N*-acetylneuraminic acid (Neu5Ac2en) for 20 min prior to data collection. Modeling of the protein and the soaked ligands was conducted in Coot[34] and further refined with REFMAC5. The resulting models were validated by Coot and MolProbity.[35] Data collection and refinement statistics are listed in Table 1.

RESULTS AND DISCUSSION

To investigate the structural and functional significance of the key amino acid residues in the active site of the AfS, three mutant enzymes, Y358H, D84A, and R171L, were constructed and expressed in *E. coli*, and their crystal structures were determined. Kinetic analysis was conducted for all enzymes,

dx.doi.org/10.1021/bi401166f | *Biochemistry* 2013, 52, 9177–9186

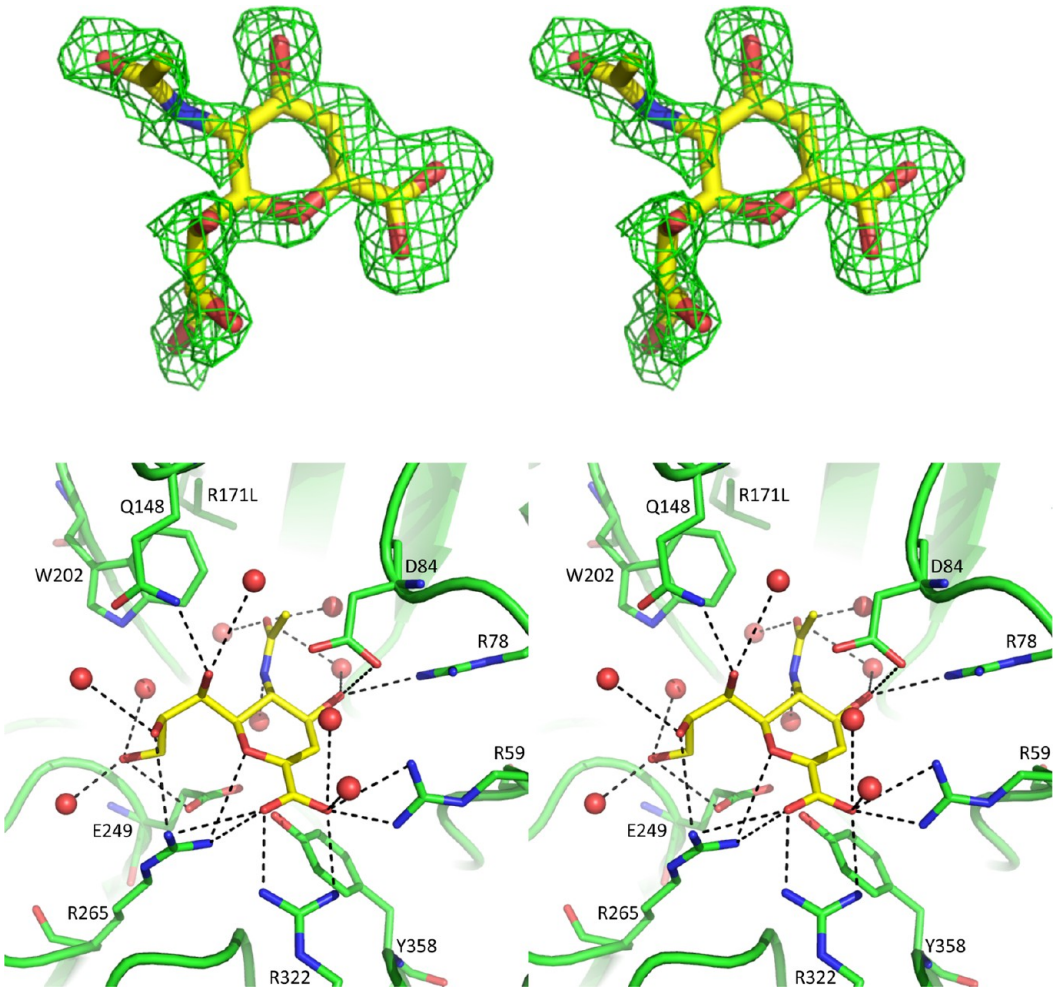

Figure 2. Crystallographic analysis of the R171L mutant in a complex with Neu5Ac2en. The top panel shows a 1.84 Å $F_o - F_c$ electron density stereoview contoured at 1.8σ for the ligand bound in monomer A of the asymmetric unit. The bottom panel shows a stereoview showing interactions of Neu5Ac2en with the active site of monomer A.

and the results were compared to the values for both wild-type AfKDNase and MvS.

pH Optima of R171L, Y358H, and D84A. Before the kinetic parameters of the mutant enzymes were determined, the pH optimum for each of the enzymes was determined, and the results are shown in Figure 2S of the Supporting Information. With 4-methylumbelliferyl α-D-KDN (KDN-MU) ($pK_a \sim 1.58$) as the substrate, the pH optimum of all mutant enzymes was 4.0, the same as for wild-type AfKDNase. The wild-type enzyme exhibited some activity at pH 5.2 (k_{cat}/K_m = 47.7 M^{-1} s^{-1}), but the nucleophilic mutant (Y358H) and the general acid/base mutant (D84A) were essentially nonfunctional at this pH. R171L was the only mutant enzyme that exhibited any activity at pH 5.2 (k_{cat}/K_m = 0.43 M^{-1} s^{-1}). In contrast, the pH optimum was 5.2 for all mutant KDNase enzymes with 4-methylumbelliferyl α-D-Neu5Ac (Neu5Ac-MU) ($pK_a \sim 1.55$) as the substrate, whereas the pH optimum was 3.5 for the wild type.[17] Unlike the wild-type enzyme for which some activity could be detected between pH 3.0 and 5.2, enzyme activity was observed at pH 5.2 only for the mutant enzymes.

Kinetic Analysis of the R171L, Y358H, and D84A Mutants of *A. fumigatus* Sialidase/KDNase. Michaelis–Menten parameters for R171L, Y358H, and D84A were measured with the following substrates: KDN-MU, Neu5Ac-MU, and KDNα2,6GalβFMU [**4** (synthesis outlined in Scheme 1 of the Supporting Information)]. The catalytic efficiency (k_{cat}/K_m) was measured for all three mutants using the three different substrates, and the data are presented in Table 2.

With KDN-MU as a substrate, R171L had a catalytic efficiency of 75.2 M^{-1} s^{-1} at pH 4.0; however, at pH 5.2, the catalytic efficiency decreased more than 2 orders of magnitude to 0.33 M^{-1} s^{-1}. The catalytic efficiencies of Y358H and D84A were 26.8 and 11.6 M^{-1} s^{-1}, respectively. At pH 5.2, Y358H and D84A had no detectable catalytic activity on KDN-MU. The catalytic efficiencies of the mutant enzymes on KDN-MU were significantly lower than that of the wild-type enzyme [k_{cat}/K_m of $(1.82 \pm 0.09) \times 10^5$ M^{-1} s^{-1}].[22] However, at pH 5.2, the wild-type enzyme has a catalytic efficiency (k_{cat}/K_m of 47.7 M^{-1} s^{-1}) similar to that of R171L at pH 4.0.

At pH values more than 0.5 pH unit from pH 5.2, the mutant enzymes cleaved Neu5Ac-MU either at a very low catalytic efficiency or at levels that were below detectable limits: at pH 4.0, the k_{cat}/K_m was 2.3 M^{-1} s^{-1} for R171L and undetectable for D84A and Y358H. In contrast, the wild-type enzyme was able to cleave Neu5Ac-MU with similar kinetic efficiency at pH 3.5 (k_{cat}/K_m = 22.3 M^{-1} s^{-1})[17] and pH 5.2 (k_{cat}/K_m = 53.3 M^{-1} s^{-1}). However, at the pH optimum of 5.2, the catalytic efficiency for the mutants with Neu5Ac-MU was within an order of magnitude of that of the wild-type enzyme: k_{cat}/K_m =

dx.doi.org/10.1021/bi401166f | *Biochemistry* 2013, 52, 9177–9186

74.2 M^{-1} s^{-1} for R171L, k_{cat}/K_m = 14.5 M^{-1} s^{-1} for Y358H, and k_{cat}/K_m = 19.0 M^{-1} s^{-1} for D84A (Table 2).

With the natural substrate analogue, KDNα2,6GalβFMU, at pH 4.0, the activity of all mutant enzymes was ~1000-fold lower than that of wild-type AfKDNase. Wild-type *A. fumigatus* KDNase had a k_{cat}/K_m of 8000 M^{-1} s^{-1}. Although the catalytic efficiencies of R171L and Y358H were similar (k_{cat}/K_m values of 1.6 and 8.9 M^{-1} s^{-1}, respectively), D84A had an even lower catalytic efficiency on KDNα2,6GalβFMU (k_{cat}/K_m of 0.2 M^{-1} s^{-1}). In this coupled enzyme reaction, the release of 8-fluoro-4-methylumbelliferone by β-galactosidase was not rate-determining for KDNα2,6GalβFMU because the concentration of β-galactosidase did not affect the rate (data not shown). We compared the ratios of the catalytic efficiencies of KDN-MU and KDNα2,6GalβFMU for the wild-type enzyme and the mutant enzymes: that of the wild-type enzyme was 22.8 ± 2.0, and the ratios for the mutant enzymes were 46.4 ± 4.9 (R171L), 3.01 ± 0.14 (Y358H), and 58 ± 29 (D84A). These observations rule out contamination of mutant enzymes by WT because mutant enzymes containing a small amount of WT would yield a ratio that was the same as that of WT.

Crystal Structures of R151L, Y358H, and D84A. The three-dimensional structures of the three mutants determined by X-ray crystallography to a resolution of 1.84 Å show that the changes made to either the tyrosine or the aspartic acid in the active site and the replacement of the arginine with a leucine in the C-5 hydroxyl group binding pocket did not affect the overall structure of the enzyme. All three mutant enzymes were expressed, purified, and crystallized via the same procedures that were used for the wild-type KDNase.[22]

R171L Mutant KDNase. Analysis of the AfKDNase crystal structure suggested that modification of arginine 171 to a leucine should allow accommodation of the *N*-acetyl group of Neu5Ac. A crystal structure of the mutant in the presence of the Neu5Ac-related tight binding inhibitor, Neu5Ac2en, shows that this is indeed the case (Figure 2), but the ligand was present in only one of the monomers in the asymmetric unit of the crystal and had a low occupancy (0.6) in the other. Nevertheless, expanding the binding pocket in R171L resulted in an enzyme that is 100-fold more active than a KDNase at pH 5.2, while AfS had a similar level of activity with both substrates (Table 3). At the pH optimum of 4.0, the wild type enzyme had

Table 3. Ratios of the Catalytic Efficiencies of Wild-Type KDNase and the R171L Mutant Using either KDN-MU or NANA-MU as the Substrate

	$k_{cat}/K_{m(KDN\text{-}MU)}/k_{cat}/K_{m(NANA\text{-}MU)}$	
	pH 4.0	pH 5.2
WT	8160	0.89
R151L	33	0.01

8000-fold higher activity on KDN-MU compared to R171L. Therefore, converting the arginine to a leucine made AfS a worse KDNase. These data indicate that the close interaction between the arginine in the binding pocket and the C-5 hydroxyl group of the sugar is essential for catalysis.

Previous phylogenetic analysis revealed that the *A. fumigatus* KDNase shares a common ancestor with bacterial sialidases in the phyla Actinobacteria and Bacteroidetes.[17] Previous work has shown that the sialidase from *Sphingobacterium multivorum*, a member of Bacteroidetes, is also a KDNase.[24] We predicted that other KDNases would have a steric clash with the *N*-acetyl group of Neu5Ac. We modeled the three-dimensional structures of selected known sialidases (*Clostridium perfringens*, *Streptococcus pneumoniae*, and *M. viridifaciens*) as well as putative KDNases (*Aspergillus terreus*, *Trichophyton rubrum*, and *Trichophyton equinum*, *Sphingobacterium* sp. 21, and *Streptomyces avermitilis*) with *A. fumigatus* KDNase. From the structures, arginine was found in all of the putative KDNases at the same position in the active site as R171, whereas in the known sialidases, the amino acid residue interacting with the *N*-acetyl group was serine. ClustalW2 alignments showed that in each case, the putative KDNases had an arginine at the same position in the sequence (Figure 3S of the Supporting Information). Experimental validation will be required to confirm the preferred substrate of these enzymes.

The cavity around the *N*-acetyl group of Neu5Ac2en is certainly larger in the R171L mutant than in the wild type (Figure 3A,B); however, the indole ring of W202 is only 3 Å

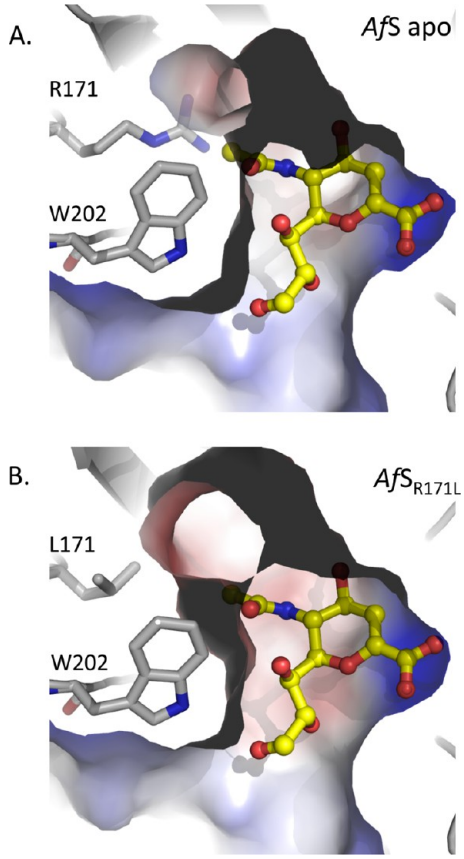

Figure 3. Effects of mutations on the cavity around C-5 of the ligand. In both images, Neu5Ac2en is modeled from the superposition of an MvS−Neu5Ac2en structure on AfS. (A) Wild-type AfS showing the clash with R171. (B) Structure of the R171L mutant showing a slightly larger cavity.

from the Neu5Ac2en methyl group, and this suggests that the mutation of W202 to a smaller hydrophobic amino acid might open the cavity further.

Y358H Mutant KDNase. The removal of the catalytic nucleophile reduced the activity of AfS by more than 1000-fold compared to that of the wild type (Table 2). This result is similar to that found with the MvS tyrosine mutants (Y370A, Y370D, and Y370G); in the MvS mutants, removal of the nucleophile resulted in a 10^2-fold decrease in activity. A more

dx.doi.org/10.1021/bi401166f | *Biochemistry* 2013, 52, 9177−9186

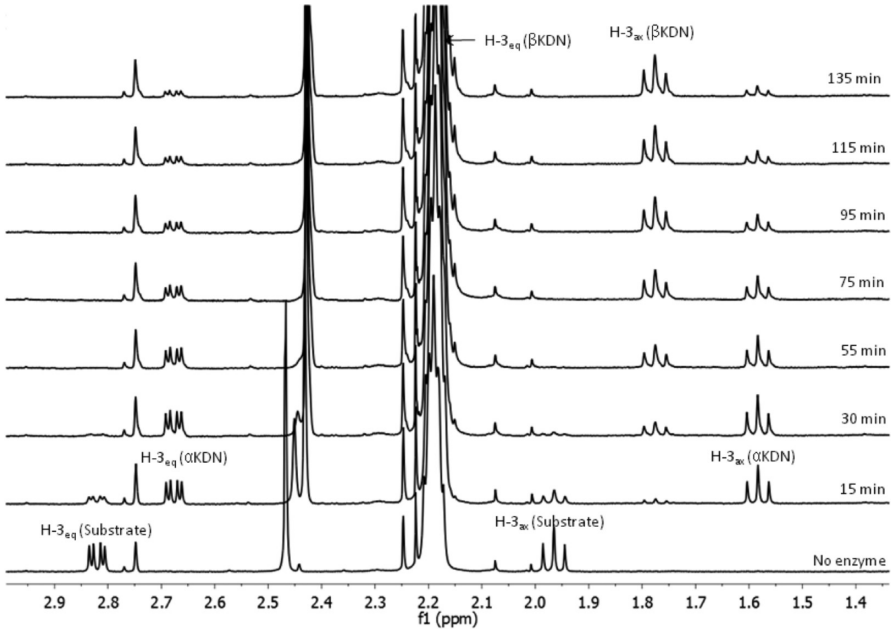

Figure 4. Y358H mutant of the AfKDNase is a retaining sialidase as determined by ^{1}H NMR. Hydrolysis of KDN-MU to form KDN was monitored over a time course. The spectra reveal the gradual depletion of the substrate followed by the production of α-KDN. The accumulation of β-KDN at 135 min results from mutarotation of α-KDN to yield the equilibrium mixture that favors the more stable β-anomer of the sugar.

profound decline (10^5-fold) in kinetic activity was found in the Y347F *Clostridium perfringens* small sialidase compared to that of the wild type[36] and in the *Trypanosoma cruzi* Y342F and Y342T mutants in which activity was eliminated.[28]

The replacement of the nucleophilic tyrosine in the MvS active site with a small negatively charged or hydrophobic side chain altered the mechanism of the enzyme by turning it into an inverting sialidase.[26] In contrast, the *A. fumigatus* Y358H mutant enzyme remains an active retaining KDNase (Figure 4). The hydrolysis of KDN-MU to form KDN was monitored as a time course reaction using ^{1}H NMR spectroscopy in deuterated buffer at pD 4.0. The $H3_{eq}$ proton of αKDN-MU showed the characteristic doublet of doublets (δ 2.82, $J_{3e,3a}$ = 12.7 Hz, $J_{3e,4}$ = 4.7 Hz). As seen in the first spectrum recorded after the addition of enzyme, an upfield chemical shift occurs for the $H3_{eq}$ resonance of the initial hydrolysis product (δ 2.68) resulting from cleavage of the umbelliferyl leaving group (Figure 4). Over time, αKDN mutarotates to the equilibrium mixture that favors the thermodynamically more stable βKDN with the appearance of the $H3_{eq}$ resonance at δ 2.20. The structure of the Y358H mutant showed little change from that of the wild type (Figure 5A,B). As can be clearly seen in the crystal structure, the replacement of the tyrosine with a histidine residue results in substitution of the nucleophilic oxygen with a more distal nitrogen atom (Figure 5D). Although histidine may act as a nucleophile, in the deglycosylation step (hydrolysis of the enzyme-bound intermediate) for the wild-type enzyme the tyrosinyl leaving group (with catalysis by the glutamate) is a good leaving group whereas the histidinyl (even when protonated) is a much worse leaving group. Only extensive isotope studies would reveal whether His is acting as a nucleophile or whether the reaction proceeds via a carbocation. This result, when taken with the decrease in activity of the Y358H mutant (6300-fold for KDN-MU), suggests that some transition state stabilizing for glycosylation by AfS results from weak nucleophilic attack occurring on the anomeric center of the KDN substrate by the tyrosine but likely none by the histidine residue. In other words, moving the nucleophilic group farther away likely changed the mechanism to a dissociative S_N1 reaction. It is known that the lifetime of an *N*-acetylneuraminylium ion, which is $>3 \times 10^{-11}$ s^{-1} (sialic acid cation),[37] is at least 10-fold longer than that for a glucopyranosylium ion[38] and that a glucopyranosylium ion is a viable intermediate in non-nucleophilic environments.[39,40] As a result, we conclude that the YH mutant AFS could operate via a dissociative S_N1 mechanism in a fashion similar to that of the Mv sialidase Y370F mutant.[41] Alternatively, it is possible that the glutamate residue changes its function from acid/base to nucleophilic catalysis. Again detailed kinetic isotope effect studies would be required to confirm this point.

D84A Mutant KDNase. The third catalytic residue in the enzyme active site is the conserved aspartic acid residue that acts as a general acid/base catalyst. Mutation of this amino acid to alanine in AfKDNase decreased its activity by 15000−50000-fold. The effect of altering the acid/base catalyst was much more pronounced in the case of AfKDNase than it was for similar mutations made in MvS (D92G, D92A, and D92S), which resulted in an only ∼10−20-fold decline in activity,[29] and the *T. cruzi trans*-sialidase (D59A), which showed k_{cat}/K_m values similar to those of the wild-type enzyme.[42] As one can see in Figure 2B, the D84A mutation did not cause significant rearrangement of the active site of the AfKDNase (Figure 5A,C,E), a conclusion that is similar to that reached about the D92G mutation in MvS.[29] Together, these data suggest that the general acid/base is more important catalytically in the reactions of the *A. fumigatus* KDNase than it is for Mv sialidase. It is possible that this phenomenon is related to the lower pH optimum of the *A. fumigatus* enzyme (pH 4.0), where the general acid residue will have a greater degree of protonation than that of the sialidase from *M. viridifaciens* (pH 5.2)[26] or the *trans*-sialidase from *T. cruzi* (pH 7.6).[42]

dx.doi.org/10.1021/bi401166f | *Biochemistry* 2013, 52, 9177−9186

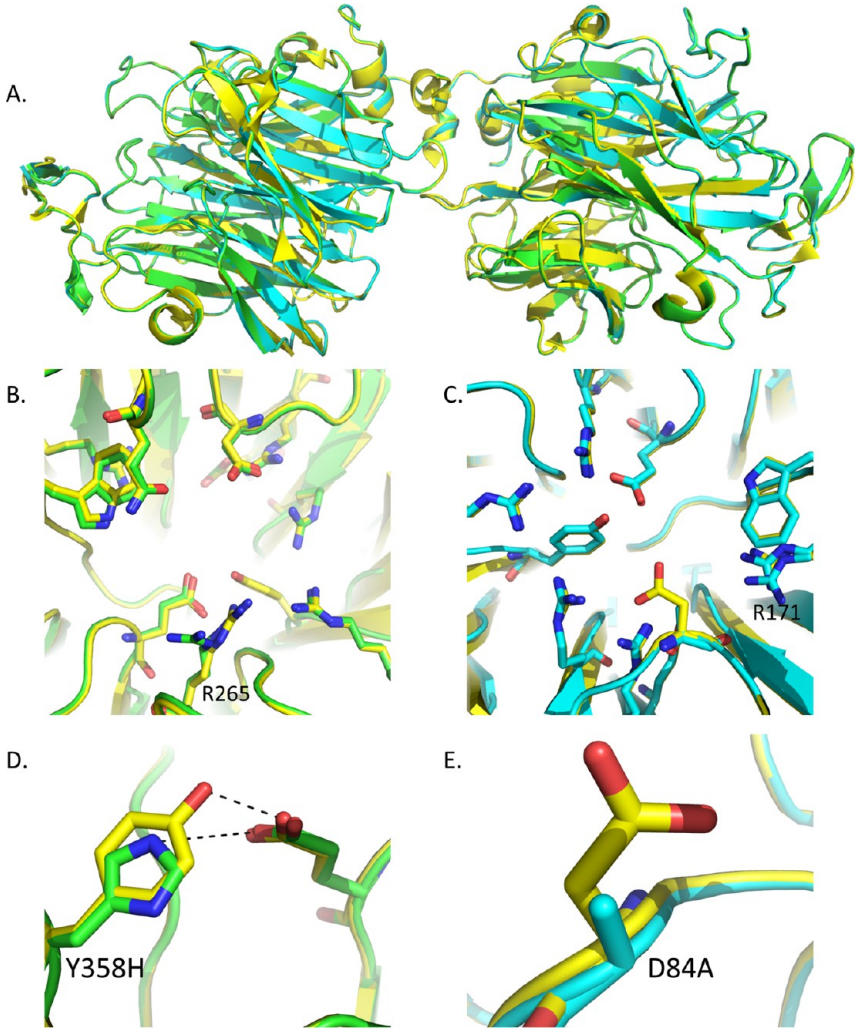

Figure 5. Crystal structures of the Y358H and D84A mutants. (A) Overlay of the two molecules in the asymmetric unit of AfS_{Y358H} (green), AfS_{D84A} (blue), and the wild type (yellow). There is no significant difference in the active site residues in the active site of either AfS_{Y358H} (B) or AfS_{D84A} (C). There are dual conformations seen for Arg265 in AfS_{Y358H} (B) and Arg171 in AfS_{D84A} (C), neither of which is likely to affect substrate binding. (D) The imidazole ring of His358 of AfS_{Y358H} superimposes over the hydroxyphenyl ring of Tyr358 of the wild-type enzyme. (E) Overlay of AfS_{D84A} with the wild-type enzyme focusing on the mutation.

CONCLUSIONS

Structure can often help predict function. A single amino acid change to enlarge the binding pocket in the R171L mutant converted the AfKDNase into a more efficient sialidase. However, the activity of the R171L mutant is still significantly lower with sialic acid as a substrate than KDN; therefore, additional amino acid changes will be necessary to accommodate the *N*-acetyl group of sialic acid. We hypothesize that an additional mutation to reduce the size of tryptophan 202 would most likely improve the sialidase activity of the AfKDNase (Figure 3C). Despite the close structural similarity of the active sites of the *A. fumigatus* KDNase with the bacterial sialidase from *M. viridifaciens*, mutants of two active site residues generated different results with the two enzymes. For example, unlike the *M. viridifaciens* sialidase and *T. cruzi trans*-sialidase in which mutation of the active site tyrosine changed the enzyme from a retaining to an inverting sialidase, the Y358H mutant of AfKDNase remained a retaining sialidase. In addition, the Y358H mutant retained appreciable enzymatic activity, unlike the protozoan enzyme for which the mutation of the nucleophile eliminated catalytic activity. Because the optimal pH of AfKDNase is 4.0, lower than those of other known sialidases, it was not unexpected that mutation of the acid in the catalytic center (D84A) caused a decrease in the activity of AfKDNase greater than that caused by aspartate mutations in the *M. viridifaciens* sialidase or *T. cruzi trans*-sialidase. These data represent the first detailed kinetic analysis of any KDNase and improve our understanding of the influences that active site structure have on sialidase activity and substrate selectivity.

ASSOCIATED CONTENT

Supporting Information

Supporting Information may be accessed free of charge online at http://pubs.acs.org.This material is available free of charge via the Internet at http://pubs.acs.org.

AUTHOR INFORMATION

Corresponding Author

*Department of Biological Sciences, Simon Fraser University, 8888 University Drive, Burnaby, BC V5A 1S6, Canada. E-mail:

mmoore@sfu.ca. Telephone: (778) 782-3441. Fax: (778) 782-3496.

Funding

We thank the Natural Sciences and Engineering Research Council of Canada (NSERC) (M.M.M. and A.J.B.), the Scottish Structural Proteomics Facility at St. Andrews, the Biotechnology and Biological Sciences Research Council, the Wellcome Trust, and the Scottish Funding Council (G.L.T.) for financial support. We thank members of the Craig laboratory (SFU) for assistance with FPLC. J.H.F.Y is a recipient of a PGSD award from NSERC.

Notes

The authors declare no competing financial interest.

REFERENCES

(1) Brakhage, A. (2005) Systemic fungal infections caused by *Aspergillus* species: Epidemiology, infection process and virulence determinants. *Curr. Drug Targets 6*, 875−886.

(2) Latgé, J.-P. (2001) The pathobiology of *Aspergillus fumigatus*. *Trends Microbiol. 9*, 382−389.

(3) Dagenais, T. R. T., and Keller, N. P. (2009) Pathogenesis of *Aspergillus fumigatus* in Invasive Aspergillosis. *Clin. Microbiol. Rev. 22*, 447−465.

(4) Wasylnka, J. A., Simmer, M. I., and Moore, M. M. (2001) Differences in sialic acid density in pathogenic and non-pathogenic *Aspergillus* species. *Microbiology 147*, 869−877.

(5) Warwas, M. L., Watson, J. N., Bennet, A. J., and Moore, M. M. (2007) Structure and role of sialic acids on the surface of *Aspergillus fumigatus* conidiospores. *Glycobiology 17*, 401−410.

(6) Severi, E., Hood, D. W., and Thomas, G. H. (2007) Sialic acid utilization by bacterial pathogens. *Microbiology 153*, 2817−2822.

(7) Vimr, E. R., Kalivoda, K. A., Deszo, E. L., and Steenbergen, S. M. (2004) Diversity of Microbial Sialic Acid Metabolism. *Microbiol. Mol. Biol. Rev. 68*, 132−153.

(8) Peterson, D. C., Arakere, G., Vionnet, J., McCarthy, P. C., and Vann, W. F. (2011) Characterization and acceptor preference of a soluble meningococcal group C polysialyltransferase. *J. Bacteriol. 193*, 1576−1582.

(9) Alviano, C. S., Travassos, L. R., and Schauer, R. (1999) Sialic acids in fungi: A minireview. *Glycoconjugate J. 16*, 545−554.

(10) Oda, L. M., Kubelka, C. F., and Alviano, C. S. (1983) Ingestion of yeast forms of *Sporothrix schenckii* by mouse Ingestion of Yeast Forms of *Sporothrix schenckii* by Mouse Peritoneal Macrophages. *Infect. Immun. 39*, 497−504.

(11) Rodrigues, M. L., Rozental, S., Couceiro, J. N. S. S., Angluster, J., Alviano, C. S., and Travassos, L. R. (1997) Identification of N-acetylneuraminic acid and its 9-O-acetylated derivative on the cell surface of *Cryptococcus neoformans*: Influence on Fungal Identification of N-Acetylneuraminic Acid and Its 9-O-Acetylated Derivative on the Cell Surface of Cryptococcu. *Infect. Immun. 65*, 4937−4942.

(12) Triglia, T., Duraisingh, M. T., Good, R. T., and Cowman, A. F. (2005) Reticulocyte-binding protein homologue 1 is required for sialic acid-dependent invasion into human erythrocytes by *Plasmodium falciparum*. *Mol. Microbiol. 55*, 162−174.

(13) Friedrich, N., Matthews, S., and Soldati-Favre, D. (2010) Sialic acids: Key determinants for invasion by the Apicomplexa. *Int. J. Parasitol. 40*, 1145−1154.

(14) Johnston, J. W., Zaleski, A., Allen, S., Mootz, J. M., Armbruster, D., Gibson, B. W., Apicella, M. A., and Munson, R. S. (2007) Regulation of sialic acid transport and catabolism in *Haemophilus influenzae*. *Mol. Microbiol. 66*, 26−39.

(15) Heikema, A. P., Bergman, M. P., Richards, H., Crocker, P. R., Gilbert, M., Samsom, J. N., Van Wamel, W. J. B., Endtz, H. P., and Van Belkum, A. (2010) Characterization of the specific interaction between sialoadhesin and sialylated *Campylobacter jejuni* lipooligosaccharides. *Infect. Immun. 78*, 3237−3246.

(16) Tiralongo, J., Wohlschlager, T., Tiralongo, E., and Kiefel, M. J. (2009) Inhibition of *Aspergillus fumigatus* conidia binding to extracellular matrix proteins by sialic acids: A pH effect? *Microbiology 155*, 3100−3109.

(17) Warwas, M. L., Yeung, J. H. F., Indurugalla, D., Mooers, A. O., Bennet, A. J., and Moore, M. M. (2010) Cloning and characterization of a sialidase from the filamentous fungus, *Aspergillus fumigatus*. *Glycoconjugate J. 27*, 533−548.

(18) Corfield, T. (1992) Bacterial sialidases: Roles in pathogenicity and nutrition. *Glycobiology 2*, 509−521.

(19) Corfield, A. P., Wagner, S. A., O'Donnell, L. J., Durdey, P., Mountford, R. A., and Clamp, J. R. (1993) The roles of enteric bacterial sialidase, sialate O-acetyl esterase and glycosulfatase in the degradation of human colonic mucin. *Glycoconjugate J. 10*, 72−81.

(20) Alviano, D. S., Franzen, A. J., Travassos, L. R., Holandino, C., Rozental, S., Ejzemberg, R., Alviano, S., Rodrigues, M. L., and Alviano, C. S. (2004) Melanin from *Fonsecaea pedrosoi* Induces Production of Human Antifungal Antibodies and Enhances the Antimicrobial Efficacy of Phagocytes. *Infect. Immun. 72*, 229−237.

(21) Uchida, Y., Tsukada, Y., and Sugimori, T. (1974) Production of microbial neuraminidases induced by colominic acid. *Biochim. Biophys. Acta 350*, 425−431.

(22) Telford, J. C., Yeung, J. H. F., Xu, G., Kiefel, M. J., Watts, A. G., Hader, S., Chan, J., Bennet, A. J., Moore, M. M., and Taylor, G. L. (2011) The *Aspergillus fumigatus* sialidase is a 3-deoxy-D-*glycero*-D-*galacto*-2-nonulosonic acid hydrolase (KDNase): Structural and mechanistic insights. *J. Biol. Chem. 286*, 10783−10792.

(23) Inoue, S., and Kitajima, K. (2006) KDN (deaminated neuraminic acid): Dreamful past and exciting future of the newest member of the sialic acid family. *Glycoconjugate J. 23*, 277−290.

(24) Nishino, S., Kuroyanagi, H., Terada, T., Inoue, S., Inoue, Y., Troy, F. A., and Kitajima, K. (1996) Induction, localization, and purification of a novel sialidase, deaminoneuraminidase (KDNase), from *Sphingobacterium multivorum*. *J. Biol. Chem. 271*, 2909−2913.

(25) Buschiazzo, A., and Alzari, P. M. (2008) Structural insights into sialic acid enzymology. *Curr. Opin. Chem. Biol. 12*, 565−572.

(26) Watson, J. N., Dookhun, V., Borgford, T. J., and Bennet, A. J. (2003) Mutagenesis of the conserved active-site tyrosine changes a retaining sialidase into an inverting sialidase. *Biochemistry 42*, 12682−12690.

(27) Amaya, M. F., Watts, A. G., Damager, I., Wehenkel, A., Nguyen, T., Buschiazzo, A., Paris, G., Frasch, A. C., Withers, S. G., and Alzari, P. M. (2004) Structural insights into the catalytic mechanism of *Trypanosoma cruzi* trans-sialidase. *Structure 12*, 775−784.

(28) Cremona, M. L., Daniel, O. S., Frasch, A. C. C., and Campetella, O. (1995) A single tyrosine differentiates active and inactive *Tyrpanosoma cruzi* trans-sialidases. *Gene 160*, 123−128.

(29) Watson, J. N., Newstead, S., Dookhun, V., Taylor, G., and Bennet, A. J. (2004) Contribution of the active site aspartic acid to catalysis in the bacterial neuraminidase from *Micromonospora viridifaciens*. *FEBS Lett. 577*, 265−269.

(30) Chan, J., Lu, A., and Bennet, A. J. (2011) Turnover is rate-limited by deglycosylation for *Micromonospora viridifaciens* sialidase-catalyzed hydrolyses: Conformational implications for the Michaelis complex. *J. Am. Chem. Soc. 133*, 2989−2997.

(31) Karwaski, M.-F., Wakarchuk, W. W., and Gilbert, M. (2002) High-level expression of recombinant *Neisseria* CMP-sialic acid synthetase in *Escherichia coli*. *Protein Expression Purif. 25*, 237−240.

(32) Leslie, A. G. W. (2006) The integration of macromolecular diffraction data. *Acta Crystallogr. D62*, 48−57.

(33) Murshudov, G. N., Vagin, A. A., and Dodson, E. J. (1997) Refinement of macromolecular structures by the maximum-likelihood method. *Acta Crystallogr. D53*, 240−255.

(34) Emsley, P., and Cowtan, K. (2004) Coot: Model-building tools for molecular graphics. *Acta Crystallogr. D60*, 2126−2132.

(35) Lovell, S. C., Davis, I. W., Arendall, W. B., III, de Bakker, P. I., Word, J. M., Prisant, M. G., Richardson, J. S., and Richardson, D. C. (2003) Structure validation by Cα geometry: ϕ, ψ and Cβ deviation. *Proteins: Struct., Funct., Genet. 450*, 437−450.

(36) Kleineidam, R. G., Kruse, S., Roggentin, P., and Schauer, R. (2001) Elucidation of the role of functional amino acid residues of the small sialidase from *Clostridium perfringens* by site-directed mutagenesis. *Biol. Chem. 382*, 313−319.
(37) Horenstein, B. A., and Bruner, M. (1998) The *N*-acetyl neuraminyl oxecarbenium ion is an intermediate in the presence of anionic nucleophiles. *J. Am. Chem. Soc. 120*, 1357−1362.
(38) Huang, X., Surry, C., Hiebert, T., and Bennet, A. J. (1995) The hydrolysis of 2-deoxy-β-D-glucopyranosyl pyridinium salts. *J. Am. Chem. Soc. 117*, 10614−1062.
(39) Lee, S. S., Hong, S. Y., Errey, J. C., Izumi, A., Davies, G. J., and Davis, B. G. (2011) Mechanistic evidence for a front-side, S_Ni-like reaction in a retaining glycosyltransferase. *Nat. Chem. Biol. 7*, 631−638.
(40) Chan, J., Tang, A., and Bennet, A. J. (2012) A stepwise solvent-promoted S_Ni reaction of α-D-glucopyranosyl fluoride: Mechanistic implications for retaining glycosyltransferases. *J. Am. Chem. Soc. 134*, 1212−1220.
(41) Watson, J. N., Newstead, S., Narine, A., Taylor, G., and Bennet, A. J. (2005) Two nucleophilic mutants of the *Micromonospora viridifaciens* sialidase operate with retention of configuration via two different mechanisms. *ChemBioChem 6*, 1999−2004.
(42) Damager, I., Buchini, S., Amaya, M. F., Buschiazzo, A., Alzari, P., Frasch, A. C., Watts, A., and Withers, S. G. (2008) Kinetic and mechanistic analysis of *Trypanosoma cruzi* trans-sialidase reveals a classical ping-pong mechanism with acid/base catalysis. *Biochemistry 47*, 3507−3512.